



Detecting the $t\bar{b}$ Decays of a Charged Higgs Boson at a Hadron Supercollider

J.F. Gunion

Davis Institute for High Energy Physics, Dept. of Physics, U.C. Davis, Davis, CA 95616

Abstract

We demonstrate that detection of a charged Higgs boson decaying via $H^\pm \rightarrow t\bar{b}$ will be possible at the LHC in $gg \rightarrow H^- t\bar{b} + H^+ b\bar{t}$ events, provided the $H^+ \rightarrow t\bar{b}$ coupling is substantial, $m_t \gtrsim 110$ GeV, and reasonably efficient and pure b -tagging can be performed.

1. Introduction

Any extension of the simple one-doublet Higgs sector of the Minimal Standard Model (MSM) that introduces either additional doublets or one or more triplets (or both) necessarily implies that at least one pair of charged Higgs bosons must exist. Thus, a charged Higgs boson is the hallmark of a truly non-minimal Higgs sector, and in particular of two-doublet models. In contrast, the presence of more than one neutral Higgs boson could be due to additional singlet Higgs representations beyond the single MSM doublet. Consequently, the ability to detect a charged Higgs boson is crucial to exploring a non-minimal Higgs sector.

Techniques for the detection of a charged Higgs boson at a hadron supercollider are model-dependent. Charged Higgs bosons that emerge from a model with two or more doublets generally have substantial fermionic couplings. All quarks of a given charge must couple to only one of the doublets if we are to avoid flavor-changing neutral currents. In the particularly simple and attractive case of two-doublets, there are then only two possible coupling patterns, conventionally labelled as type-I and type-II. In type-II models, doublet 2 couples to up quarks while doublet 1 couples to down quarks.^[1] Defining $\tan\beta \equiv v_2/v_1$, the ratio of the vacuum expectation values of the neutral members of the two doublets, the resulting $H^+ \rightarrow t\bar{b}$ coupling is given by^{*}

$$\frac{g}{\sqrt{2}m_W} [m_b P_{RB} + m_t P_{LT}] \quad (1)$$

with $B = \tan\beta$ and $T = \cot\beta$, where $P_{(R,L)} = \frac{1}{2}(1 \pm \gamma_5)$. The two-doublet Higgs sector of the Minimal Supersymmetric Model (MSSM) is necessarily of this type. In models of type-I, only doublet 2 has quark couplings; doublet 1 couples only to vector bosons at tree-level. The resulting $H^+ \rightarrow t\bar{b}$ coupling is obtained from Eq. (1) by setting $T = -B = \cot\beta$.

Models with Higgs triplets alone cannot yield $\rho \equiv m_W/(m_Z \cos\theta_W) = 1$ nor can they provide a source for fermion masses. The simplest model that yields $\rho = 1$ at tree-level

* A b -quark mass of $m_b(2m_b) = 4.7$ GeV is employed here and elsewhere in our computations.



consists of one $Y = 1$ doublet, one $Y = 0$ real triplet and one $Y = 2$ complex triplet.^[1] The Higgs mass eigenstates include two charged Higgs bosons, one of which (H_3^+ in the standard notation) couples to $t\bar{b}$ according to Eq. (1) with $T = -B = \tan \theta_H$, where $\tan \theta_H$ characterizes the ratio of triplet vev's to the vev of the neutral member of the doublet field. The larger the role of the triplets in giving mass to the W^\pm and Z , the larger $\tan \theta_H$. The other charged Higgs boson of this model (H_5^+) couples strongly to W^+Z when $\tan \theta_H$ is large, and is generally quite easily produced by W^+Z fusion and detected in the W^+Z final state.^[1] This letter focuses on the seemingly more challenging problem of developing techniques allowing the detection of a charged Higgs boson with no tree-level W^+Z coupling, but with substantial fermionic couplings.

In Refs. 2 and 3 it was demonstrated that detection of $t \rightarrow H^+b$ decays, by searching for a violation of τ -lepton universality, would be relatively straightforward. In contrast, it has generally been thought that detection of an H^+ which decays predominantly to $t\bar{b}$ would not be possible at a hadron collider. In this letter, we demonstrate that b -tagging should allow detection of this decay mode for a substantial range of top quark masses and $H^+ \rightarrow t\bar{b}$ coupling strengths.^[4]

2. Procedure and Results

The techniques employed are closely related to those developed for detection of $t\bar{t} + h$ with $h \rightarrow b\bar{b}$.^[5] Indeed, the $t\bar{t}b\bar{b}$ final state resulting from $gg \rightarrow t\bar{t}H^- + \bar{t}bH^+$ (followed by $H^\pm \rightarrow tb$) is precisely the same and the same backgrounds — $gg \rightarrow t\bar{t}b\bar{b}$, $gg \rightarrow t\bar{t}Z$ with $Z \rightarrow b\bar{b}$, and $t\bar{t} + jets$ — must be brought under control. The large size of the $t\bar{t} + jets$ background implies that the ability to tag three or more b -jets with good efficiency and purity will almost certainly be required.

Note that we shall generate signal and backgrounds as initiated by gg collisions. If precisely three b -quarks are tagged, then an alternative treatment can be envisioned in which one studies H^\pm detection using the process $g\bar{b} \rightarrow \bar{t}H^+ \rightarrow \bar{t}t\bar{b}$ and its charge conjugate for the signal and related $2 \rightarrow 3$ reactions for the backgrounds. However, this $2 \rightarrow 3$ procedure obscures the fact that there really is a second b -quark (associated with the colliding \bar{b} above) that could be tagged. The $2 \rightarrow 4$ procedure adopted here will better reflect the full kinematics of the underlying production reaction in the types of high-transverse momentum configurations in which it is probed; in particular, it will allow one of the b -tags to be supplied by the b -quark which is an 'invisible' spectator in the $2 \rightarrow 3$ procedure. It will also yield a more reliable representation of the full complexity of the multi-jet environment in which one must achieve the required isolations for multiple b -tagging. Finally, it will more accurately include combinatoric background effects. The only short-fall of the $2 \rightarrow 4$ procedure is that it will generally underestimate the actual cross section magnitudes. This is well-understood^[6] as being due to the absence of the leading-log development of QCD radiation from the final state b -quarks in the tree-level $2 \rightarrow 4$ computation that is implicitly included in defining the b -quark distribution employed in the $2 \rightarrow 3$ technique. Thus, it will be necessary to multiply our $2 \rightarrow 4$ results by significant QCD correction factors (to be specified below) in order to reproduce correctly the cross section values. These QCD correction factors were estimated by simply comparing the uncut $2 \rightarrow 4$ cross section with the uncut $2 \rightarrow 3$ cross section for the reactions of interest.

Of course, the $2 \rightarrow 3$ cross sections will, themselves, have higher order QCD corrections. These are not available in the literature and are not computed here. However, there is one component of the QCD corrections to the H^\pm production process that will almost certainly emerge in the full QCD-correction computation. Namely, it is reasonable to anticipate that the QCD-corrected H^\pm production cross section will approximately factorize into a fairly constant overall K factor (presumably significantly larger than 1 for our gg -induced production mechanism, but taken equal to 1 for the numerical results of this paper) times the lowest order result with the $H^+ \rightarrow t\bar{b}$ coupling expressed in terms of running quark masses. Indeed, in the closely related computation of the QCD corrections to the $H^+ \rightarrow t\bar{b}$ width,^[7] replacing the physical quark masses by running masses yields an excellent approximation to the full result. In the present computation we refer all quark masses to their values at quark pair production threshold, $m_f(2m_f)$. This implies that the running t -quark mass is slightly larger (smaller) than the physical threshold t -quark mass for m_{H^+} below (above) $2m_t$, whereas, since m_{H^+} is always much larger than $2m_b$, the running b -quark mass is always significantly smaller than the physical b mass (typically by a factor of order 0.77). Thus, in models of type-II, inclusion of running mass corrections will significantly decrease the H^\pm production cross section compared to its uncorrected value when the m_b term in the $H^+ \rightarrow t\bar{b}$ coupling is dominant, *i.e.* when $\tan\beta$ is large.

We now give additional details on the precise procedures followed. We use the MRS-D0' distribution functions^[8] evaluated at a momentum scale given by the subprocess center-of-mass energy. We adopt an energy of $\sqrt{s} = 16$ TeV for the LHC. All jet and lepton momenta are smeared using resolutions of $\Delta E/E = 0.5/\sqrt{E} \oplus 0.03$ and $\Delta E/E = 0.2/\sqrt{E} \oplus 0.01$, respectively (\oplus means added in quadrature). An isolated lepton (e or μ) from one t decay is used as the trigger. The lepton is required to have $p_T > 20$ GeV, $|\eta| < 2.5$ and to be separated by $\Delta R > 0.3$ from the nearest lepton or jet. A missing energy of $|\vec{p}_T^{\text{miss}}| > 50$ GeV is required. At least three jets must be found in the $|\eta| < 2.5$ region with $p_T > 30$ GeV. (To be declared a jet, a quark or gluon must be separated by $\Delta R > 0.7$ from its nearest neighbor.) Three tagged b -jets are then required. Only b -jets (and, when mis-tagged, other jets) with $|\eta| < 2$ and $p_T > 20$ GeV, isolated from any other tagged jet by $\Delta R > 0.5$, are considered. Within these kinematic restrictions, the probability for tagging a true b -jet is taken to be that found in the SDC detector Technical Design Report,^[9] which gives $e_{b\text{-tag}}$ for the vertex detector as a function of the p_T of the b -jet. (Including tagging of semi-leptonic b decays via a lepton with significant p_T relative to the main jet direction would add to this efficiency.) In this same kinematic range, the probability for mis-identifying a regular gluon or light quark jet as a b -jet, $e_{\text{mis-id}}$, is taken to be 0.01, which is representative of the values obtained in Ref. 9, while the probability of mis-tagging a c -jet is taken to be 0.05. We do not have available similar results for the LHC detectors. It might prove that these $e_{b\text{-tag}}$ and $e_{\text{mis-id}}$ values are optimistic given the multiple interactions that occur in a given crossing when the LHC is run at high instantaneous luminosity.

Additional cuts delineated below tend to require that the second W from t decay must decay hadronically, and that this W combine with a tagged b -jet to form a top quark. More precisely, the invariant mass of each pair of jets, M_{jj} , is computed and at least one pair *not containing any tagged b -quark* is required to have $m_W - \Delta m_W/2 \leq M_{jj} \leq m_W + \Delta m_W/2$. In addition, each pair of jets satisfying this criteria is combined with each of the tagged b -jets to compute the three-jet invariant mass, M_{bjj} . $m_t - \Delta m_t/2 \leq M_{bjj} \leq m_t + \Delta m_t/2$

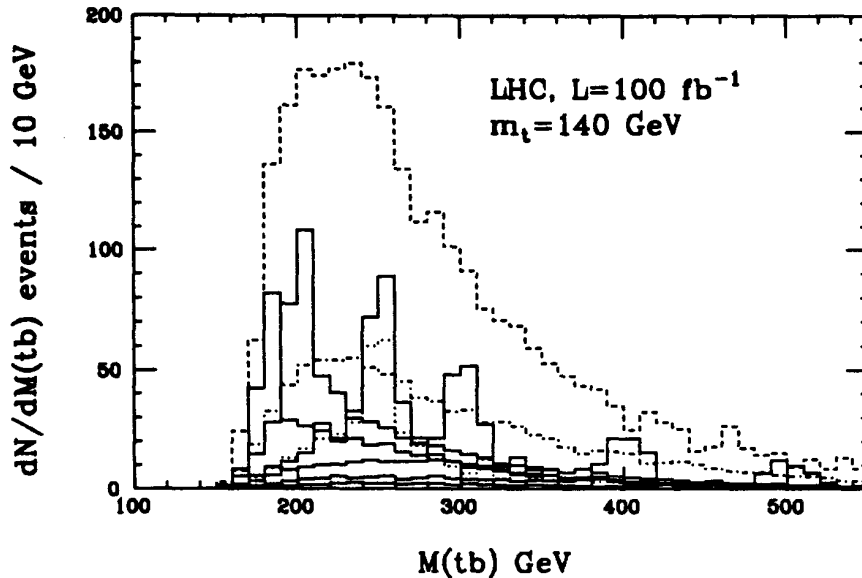


Figure 1: dN/dM_{bbj} is plotted as a function of M_{bbj} for: the $gg \rightarrow b\bar{t}H^+ + \bar{b}tH^-$ signal (solid); the $gg \rightarrow t\bar{t}b\bar{b}$ background (dot-dash); and the $t\bar{t}g$ mis-tagged background (dashes). For this plot we have employed the type-II two-doublet coupling with $\tan\beta = 1$, $m_t = 140$ GeV, and an integrated luminosity of $L = 100 \text{ fb}^{-1}$ at the LHC. Signal curves are given for $m_{H^+} = 180, 200, 250, 300, 400$ and 500 GeV. Results do not include any QCD K-factors for the $t\bar{b}H^\pm$ signal or $t\bar{t}b\bar{b}$ background. No additional K-factor for the $t\bar{t}g$ background is appropriate. QCD corrections to the $H^+ \rightarrow t\bar{b}$ vertex are also not included. For the solid signal curves, semi-leptonic decays of the b -quarks are not included. The effect of their inclusion is illustrated in the case of the $m_{H^+} = 250$ GeV signal by the dotted histogram.

is then required for at least one bjj combination. If mass cuts of $\Delta m_W = 15$ GeV and $\Delta m_t = 25$ GeV are used, only a small fraction of signal events are eliminated for the earlier-quoted jet and lepton energy resolutions, whereas the reducible backgrounds are significantly decreased. Finally, a plot of the M_{bbj} mass distribution is made, where both b 's are required to be tagged and the two j 's must *not* have been tagged. Typical results (before applying QCD corrections) for the M_{bbj} distribution are shown in Fig. 1. For m_{H^+} not too near the $H^+ \rightarrow t\bar{b}$ decay threshold, clear signal peaks are seen for $m_{H^+} \lesssim 400$ GeV where the H^+ production rate is significant. As m_{H^+} approaches $m_t + m_b$, the b quark from the decay of the H^+ only infrequently has sufficient p_T to be tagged, and the signal peak deteriorates.

The signal results shown by the solid curves in Fig. 1 do not include the semi-leptonic

decays of the b -quark. If no attempt to identify those tagged b -quarks that decay semi-leptonically is made, semi-leptonic decays reduce the number of events in the central charged Higgs peaks. On average, the reduction is of order 25%, part of which reduction is due to the failure to reconstruct m_t within Δm_t for events with a semi-leptonic decay of the relevant b . A sample is shown by the dotted curve for the $m_{H^+} = 250$ GeV signal. It could be that those tagged b -quarks which decay semi-leptonically can be identified by observation of the lepton within the jet. (This is certainly possible for the μ 's, and may also be possible a significant fraction of the time for e 's since they tend to have visible p_T relative to the main jet axis.) In this case, the visible momenta can be rescaled to reflect the lost neutrino momentum, so as to better reconstruct the average underlying b -quark momentum. We will not attempt this procedure here.

The only important backgrounds, after all cuts, turn out to be the $t\bar{t}b\bar{b}$ continuum QCD background, and $t\bar{t}g$ where the g is mis-tagged (with 1% probability) as a b -jet. The $t\bar{t}Z$, with $Z \rightarrow b\bar{b}$, background is much smaller than either. For a mis-identification probability of 0.05 for a c -quark, the $t\bar{t}c\bar{c}$ background is also not significant. Intuitively, this can be understood by noting that the $t\bar{t}b\bar{b}$ and $t\bar{t}c\bar{c}$ cross sections are not very different once the tagged b or c is required to have significant transverse momentum, whereas the probability for tagging a b is much higher (a factor of 6) on average. Finally, we note that including semi-leptonic decays leads to background distributions that are about 10% smaller than those illustrated in Fig. 1.

Before the significance of such signals can be computed, we must apply appropriate QCD correction factors as explained earlier. We have employed a K -factor of 2 for the $gg \rightarrow t\bar{t}H^- + \bar{t}bH^+$ signal, and the $gg \rightarrow t\bar{t}Z$ and $gg \rightarrow t\bar{t}b\bar{b}$ backgrounds. The $t\bar{t}g$ background has been computed employing a cutoff of $p_T > 30$ GeV for the final state g . As explained in Ref. 5, this yields a $t\bar{t}g$ total cross section that is 60% of the $t\bar{t}$ leading order cross section. Thus, by computing the $t\bar{t}g$ process with this cutoff, the effective K factor for $t\bar{t}$ production of $K = 1.6$ is reproduced. Finally, the corrections to the $H^+ \rightarrow t\bar{b}$ vertex due to the running of the quark masses are applied.

Table 1: Number of 100 fb^{-1} years, Y , (signal event rate, S) at LHC required for a 5σ confidence level charged Higgs signal in a 40 GeV wide mass interval centered about m_{H^+} , assuming 3 jets are tagged as b 's and $e_{\text{mis-tag}} = 1.0\%$.

$BR(H^+ \rightarrow t\bar{b}) = 1$ and model-II couplings with $\tan\beta = 1$ are assumed.

$m_t =$	m_{ϕ^0}	150	170	200	250	300	400
110	$Y(S)$	4.7(179)	1.8(151)	2.6(196)	2.8(159)	2.7(115)	6.6(105)
$m_t =$	m_{ϕ^0}	180	200	250	300	400	500
140	$Y(S)$	0.6(93)	0.5(115)	0.5(121)	0.6(102)	1.3(89)	2.1(72)
$m_t =$	m_{ϕ^0}	200	220	250	300	400	500
180	$Y(S)$	25.5(243)	0.3(52)	0.2(60)	0.3(71)	0.6(69)	1.1(65)

To estimate the statistical significance, N_{SD} , of a charged Higgs signal we compute the signal event rate S by focusing on either two or four 10 GeV bins centered about m_{H^+} (generally four bins is optimum, but for m_{H^+} close to the $t\bar{b}$ decay threshold two bins gives the best statistical significance). The combinatoric background from the signal reaction itself is estimated using the bins immediately beyond the central bins, and is then subtracted from the central bins. S is then computed by summing the remainder event rate over the two or four central bins. The background B in this same mass interval is computed by summing all the background rates, including the combinatoric signal background subtracted in obtaining S , over the same central bins. We then compute $N_{SD} = S/\sqrt{B}$. The results, after including semi-leptonic b decays, are presented in Table 1, in terms of the number of LHC 100 fb⁻¹ years (Y) required to detect a given charged Higgs signal at the 5 sigma level. Also given is the signal event rate (S) for this number of years. The corresponding background rate can be obtained by the relation $B = (S/5)^2$. Table 1 assumes model-II coupling with $\tan\beta = 1$, and gives results for four bins of combined width 40 GeV. For the lowest m_{H^+} values considered for each m_t , better results are actually obtained if a two-bin, *i.e.* 20 GeV, interval is employed. For a 20 GeV interval we find $Y(S) = 2.1(81)$, $0.4(60)$ and $5.6(65)$ for $[m_t, m_{H^+}] = [110, 150]$, $[140, 180]$, and $[180, 200]$, respectively. All are improvements over the four-bin results of Table 1. Overall, we see that a charged Higgs boson with substantial $H^+ \rightarrow t\bar{b}$ coupling and mass not too close to the $t\bar{b}$ decay threshold can be readily detected at the LHC using b -tagging. Since the largest background is that from $t\bar{t}g$, with the g mis-tagged as a b -quark, the clarity of the H^\pm signals would be significantly increased by improving the tagging purity to $e_{mis-tag} \lesssim 0.005$,

The actual $H^+ \rightarrow t\bar{b}$ coupling may be either greater or smaller than that obtained in model-II with $\tan\beta = 1$. In model-II, the effective coupling strength decreases rapidly as $\tan\beta$ increases, reaching an m_t (and m_b) dependent minimum in the $\tan\beta \sim 5 - 7$ region, and then rises rapidly as $\tan\beta$ increases further, thereby leading to a greatly enhanced m_b coefficient. This behavior is illustrated in Fig. 2, where we plot the effective coupling strength defined by $g_{eff}^2 \equiv (m_t^2 T^2 + m_b^2 B^2)/(m_t^2 + m_b^2)$, the denominator being the coupling strength squared for $T = B = 1$, *i.e.* $\tan\beta = 1$.^{*} In Fig. 2 we use $m_b = 3.6$ GeV which is a typical value for the running b -quark mass at moderate m_{H^+} . Although not plotted, it is apparent that g_{eff}^2 rises rapidly above 1 for $\tan\beta < 1$.

This behavior can potentially affect our results in two ways. First, it could, in principle alter $BR(H^+ \rightarrow t\bar{b})$ which we have assumed to be near unity in Table 1. However, even at the minimum, the $H^+ \rightarrow t\bar{b}$ coupling strength squared is far larger than that for any competing SM fermion-pair channel, and the branching ratio remains near unity. Second, and very crucial, since the H^+ production rate is proportional to g_{eff}^2 , N_{SD} must be multiplied by g_{eff}^2 , and $Y(S)$ in Table 1 must be divided by $g_{eff}^4(g_{eff}^2)$. Obviously, a statistically significant charged Higgs signal cannot be achieved for $\tan\beta$ near the minimum point. Viable signals may only be obtained for $\tan\beta \lesssim 2$ and large $\tan\beta$. More quantitatively, if $m_t \sim 140(180)$ GeV a 5 sigma signal is obtained in 2 - 3 LHC 100 fb⁻¹ years for $m_{H^+} \lesssim 400$ GeV

* We have checked numerically that the H^\pm cross sections are closely proportional to g_{eff}^2 . This means that the squares of the scalar and pseudoscalar couplings (there is no interference) of Eq. (1) enter the cross section with very similar weights.

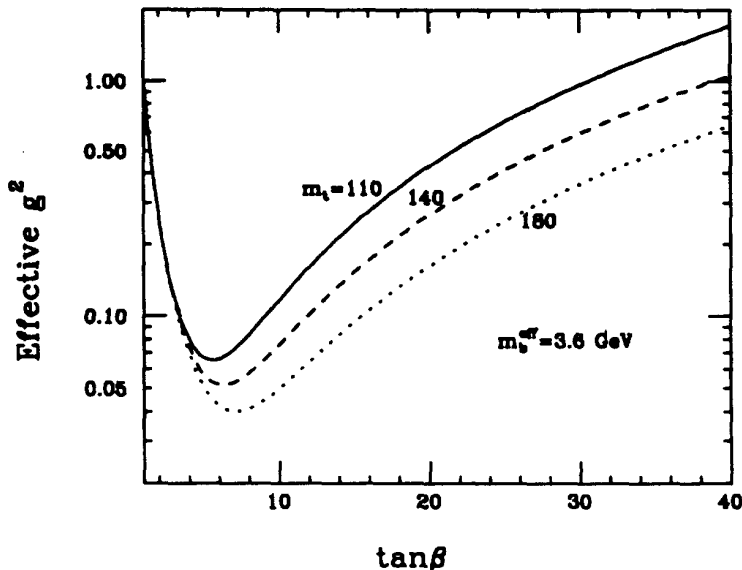


Figure 2: We plot g_{eff}^2 as a function of $\tan\beta$ for $m_t = 110, 140,$ and 180 GeV in the case of model-II coupling with $m_b = 3.6$ GeV (typical of the running b -quark mass evaluated at moderate m_{H^+}).

if $\tan\beta \lesssim 1.5(1.7)$. And, for all three m_t values a 5 sigma signal is obtained in 2 – 3 LHC years for $m_{H^+} \lesssim 300$ GeV (but not too near threshold) if $\tan\beta \gtrsim 30$.

The values of $\tan\beta$ that are of greatest interest depend upon the larger model context. In a non-supersymmetric two-doublet model of type-II, small values of $\tan\beta$ tend to be excluded, for the m_{H^+} values considered here, by the experimental upper limit on the $b \rightarrow s\gamma$ branching ratio.^[10] In the MSSM (for which the Higgs sector is required to be a two-doublet model of type-II) loops involving charginos cancel against loops involving the charged Higgs, and there is no significant constraint on $\tan\beta$ coming from the experimental limit on $BR(b \rightarrow s\gamma)$.^[11] Both $\tan\beta \lesssim 2$ and $\tan\beta \gtrsim 30$ are allowed regions of parameter space, and in these regions discovery of the H^\pm will be possible in the mode explored here, assuming decays of the H^+ to chargino+neutralino states do not decrease $BR(H^+ \rightarrow t\bar{b})$ to a value significantly below 1. We note that small $\tan\beta \lesssim 2$ and very large $\tan\beta \gtrsim 40$ are the preferred regions in GUT scenarios for the MSSM in which $\lambda_b = \lambda_\tau$ is required at the GUT scale.^[12]

In the case of model-I couplings, the m_b term is not enhanced at large $\tan\beta$, and so discovery of the H^+ in the $t\bar{b}$ decay mode will be restricted to $\tan\beta \lesssim 2$ as described above for model-II. For the triplet model outlined earlier, H_3^+ discovery in the $t\bar{t}b\bar{b}$ final state will

require $\tan \theta_H \gtrsim 0.5$. However, the limit on $BR(b \rightarrow s\gamma)$ will tend to rule out $\tan \beta$ and $\tan \theta_H$ values in the above ranges, unless the models are supplemented with additional new physics that yields loop corrections which cancel against the charged Higgs loop.

3. Conclusion

In conclusion, detection of a charged Higgs boson in the $gg \rightarrow t\bar{b}H^- + \bar{t}bH^+ \rightarrow t\bar{t}b\bar{b}$ production/decay mode will be possible for a significant range of $\tan \beta$ values in a two-doublet model of type-II, which is the most attractive Higgs sector extension and, in particular, is that required in the Minimal Supersymmetric Model. Indeed, the $\tan \beta$ regions for which discovery is viable correspond precisely to those preferred when the MSSM is considered in a GUT context. In contrast, parameter choices allowing H^\pm discovery via the $t\bar{t}b\bar{b}$ mode in type-I two-doublet models and in the above-described triplet Higgs model (with custodial SU(2) symmetry at tree-level) tend to be ruled out by experimental limits on $BR(b \rightarrow s\gamma)$.

The ability to perform b -tagging with good efficiency and purity is crucial to the techniques developed here. It will be important for the LHC detectors to optimize their ability to tag b -quarks in the multi-event per collision environment that will prevail for the high instantaneous luminosity required to achieve integrated luminosities of order 100 fb^{-1} .

Acknowledgements

This work has been supported in part by Department of Energy grant #DE-FG03-91ER40674 and by Texas National Research Laboratory grant #RGFY93-330. I am grateful to M. Barnett, H. Haber, and F. Paige for helpful conversations. Some of the Monte Carlo generators employed were developed in collaboration with J. Dai, L. Orr and R. Vega.

References

1. For a review see J.F. Gunion, H.E. Haber, G.L. Kane, and S. Dawson, *The Higgs Hunter's Guide*, Addison-Wesley, Redwood City, CA (1990).
2. R.M. Barnett, R. Cruz, J.F. Gunion and B. Hubbard, *Phys. Rev. D* **47** (1993) 1048.
3. D.P. Roy, *Phys. Lett.* **B283** (1992) 403.
4. A preliminary report of the SSC results using the techniques presented here appears in J.F. Gunion and S. Geer, preprint UCD-93-32 (1993), to appear in *Proceedings of the "Workshop on Physics at Current Accelerators and the Supercollider"*, eds. J. Hewett, A. White, and D. Zeppenfeld, Argonne National Laboratory, 2-5 June (1993).
5. J. Dai, J.F. Gunion and R. Vega, *Phys. Rev. Lett.* **71** (1993) 2699.
6. See for example, J.F. Gunion *et al.*, *Nucl. Phys.* **B294** (1987) 621; F. Olness and W.-K. Tung, *Nucl. Phys.* **B308** (1988) 813; D.A. Dicus and S. Willenbrock, *Phys. Rev.* **D39** (1989) 751.
7. A. Mendez and A. Pomarol, *Phys. Lett.* **B252** (1990) 461. See, also, M. Drees and K. Hikasa, *Phys. Lett.* **B240** (1990) 455, Erratum-*ibid.* **B262** (1991) 497.
8. A.D. Martin, W.J. Stirling, and R.G. Roberts, *Phys. Lett.* **B306** (1993) 145; Erratum-*ibid.* **B309** (1993) 492.

9. Solenoidal Detector Collaboration Technical Design Report, E.L. Berger *et al.*, Report SDC-92-201, SSCL-SR-1215, 1992, p 4.15-4.16.
10. J.L. Hewett, *Phys. Rev. Lett.* **70** (1993) 1045; V. Barger, M.S. Berger, and R.J.N. Phillips, *ibid.* **70** (1993) 1368.
11. S. Bertolino, F. Borzumati, and A. Masiero, *Nucl. Phys.* **B294** (1987) 321; S. Bertolini, F. Borzumati, A. Masiero, and G. Ridolfi, *Nucl. Phys.* **B353** (1991) 591; R. Barbieri and G.F. Giudice, preprint CERN-TH 6830/93 (1993); J. Lopez, D. Nanopoulos, and G. Park, preprint CTP-TAMU-16-93 (1993); N. Oshimo, preprint IFM 12/92 (1992).
12. See, for example, V. Barger, M.S. Berger, and P. Ohmann, preprint MAD/PH/798 (1993) and references therein.